International Journal of Radiation Biology, March 2013; 89(3): 155–161

ISSN 0955-3002 print / ISSN 1362-3095 online
DOI: 10.3109/09553002.2013.734941

informa
healthcare

Electrophysiological, biochemical and ultrastructural effects of radiotherapy on normal rat sciatic nerve

Savas Aktas[1], Ulku Comelekoglu[2], S. Necat Yilmaz[1], Serap Yalin[3], Suat Arslantas[4], Banu Coskun Yilmaz[1], Fatma Sogut[2], Mehmet Berkoz[3] & Mehmet Ali Sungur[5]

Department of [1]Histology & Embryology, [2]Biophysics, [3]Biochemistry, and [5]Biostatistics Medical Informatics, Faculty of Medicine, Mersin University, Mersin, Turkey, and [4]Radiation Oncology Clinic, Adana Numune Hospital, Adana, Turkey

Abstract

Purpose: **The aim of the present study was to evaluate the electrophysiological, biochemical and ultrastructural changes on the rat sciatic nerve after radiotherapy.**

Material and Methods**: Thirty male Wistar albino rats were divided into three groups as: Control group ($n = 10$), Group I: 3 months after radiotherapy ($n = 10$), and Group II: 6 months after radiotherapy ($n = 10$). Groups I and II were irradiated with a ^{60}Co gamma source. A dose of 20 Gy in 10 fractions was applied to Groups I and II. Compound motor action potentials (CMAP) were recorded in all groups. Superoxide dismutase (SOD) and catalase (CAT) activities and malondialdehyde (MDA) levels were measured in the sciatic nerve of rats using the biochemical methods. Ultrastructural changes were determined by electron microscopy.**

Results: **In Groups I and II, the amplitude of CMAP was significantly lower and the latency was significantly higher than that of the control group. There were no significant differences between Groups I and II regarding the CMAP amplitude and latency. The MDA levels were significantly increased, whereas the SOD and CAT activities were significantly decreased in experimental groups when compared with the control group. However, there were no significant changes in these parameters between Groups I and II. Degeneration in myelinated nerve fibers was observed ultrastructurally only in the experimental groups. Significant changes were observed between the control group and experimental groups in terms of ultrastructural myelin grading score and axonal damage score. No significant differences were found between Groups I and II.**

Conclusions: **These findings indicated that the dose of 20 Gy in 10 fractions radiotherapy caused neuropathic damages in normal rat sciatic nerve 3 and 6 months after irradiation.**

Keywords: External beam radiotherapy, sciatic nerve, ultrastructure, nerve conduction, lipid peroxidation

Introduction

In conventional external beam radiotherapy (EBRT), two-dimensional beams produced by an accelerator target the tumor mass. Ionizing radiation (IR) has direct and indirect harmful effects on the cancer and surrounding healthy tissues. IR can damage DNA by ionizing directly and also indirectly by producing reactive oxygene species (ROS) around DNA (Iliakis 1991, Goodhead 1994). The destructive action of radiotherapy is predominant due to the ROS, including the superoxide radical ($O_2^{\cdot -}$), the hydroxyl radical ($OH^{\cdot}$) and hydrogen peroxide (H_2O_2), generated by the decomposition of water (H_2O) (Data et al. 2000). Superoxide dismutase (SOD) enzyme catalyzes the dismutation of $O_2^{\cdot -}$ into H_2O_2. H_2O_2 can then be transformed into H_2O and oxygen (O_2) by the enzymes catalase (CAT) and glutathione peroxidase (GSH-Px). Oxidative damage arises when rates of ROS production outpace rates of removal (Mates et al. 1999). One of the indices of oxidative damage is the level of malondialdehyde (MDA) which is formed as an end product of lipid peroxidation (Halliwell and Gutterage 1990).

Radiosensitivity of many types of tissues limits the application of high radiation doses. Despite neurons have high intrinsic resistance to radiation, the nervous system is considered vulnerable to radiation therapy. Glial cells are thought to be primarily most sensitive structures to radiation. Radiation induced neurotoxicity can involve both the central and peripheral nervous systems (Liang 1999). Radiation-induced neurotoxicity has been reported in many experimental studies. Ruifrok et al. (1992, 1994) reported that radiation of rat spinal cord causes diffuse demyelination axon swelling, focal necrosis, gliosis in white matter and paresis of the forelegs. In a study on ventral nerve roots of the rat cauda equine, demyelination, proliferation of Schwann cells and devolopment of malignant schwannoma were reported

Correspondence: Dr Savas Aktas, Mersin Universitesi, Tip Fakultesi, Çiftlikköy Kampusu, Temel Tıp Bilimleri Binası B-Blok Histoloji ve Embryoloji AD 33169 Mersin, Turkey. Tel: +90 324 3413066; Fax: +90 324 3412312. E-mail: saktas@mersin.edu.tr

(Received 14 February 2012; revised 10 September 2012; accepted 20 September 2012)

after IR (van der Kogel 1977). In another study on dog sciatic nerve, it was reported that myelinated nerve fiber loss, fibrosis of the endoneurium and hind limb paresis occurred following IR (Kinsella et al. 1985). In an experimental rat sciatic nerve study, impairment of motor functions was observed after delivering radiation (de Vrind et al. 1993). Despite many studies with IR on peripheral nerves, ultrastructural, biochemical and electrophysiological reports are inadequate on rat sciatic nerve after radiotherapy. The aim of the present study was to examine the electrophysiological, biochemical and ultrastructural changes on the rat sciatic nerve after 3 and 6 months postradiation.

Materials and methods

Animals

Thirty healthy adult male Wistar albino rats (6- to 8-week-old, average body weight 180–200 g) were used in the present study. Rats were obtained from the Experimental Animal Center, University of Mersin, Turkey. The study was approved by the research and ethical committee of the University of Mersin. The rats were housed in polycarbonate boxes (Plexx B.V., Elst, The Netherlands) (3 or 4 rats per box) with steel wire tops (Plexx B.V.) and rice husk bedding (Mehmet Barbaros Denizeri Deney Hayvanları Yem Sanayi Fabrikası, Gebze, Kocaeli, Turkey). They were maintained in a controlled atmosphere of 12 h dark/light cycle, 22 ± 2°C temperature, and 50–70% humidity, with free access to food and fresh tap water. The animals were supplied with dry food pellets (Mehmet Barbaros Denizeri Deney Hayvanları Yem Sanayi Fabrikası, Gebze, Kocaeli, Turkey) commercially available. The animals were randomly assigned into three groups each consisting of 10 rats: The control group, Group I (3 months after irradiation) and Group II (6 months after irradiation).

Radiotherapy

Prior to irradiation, the two experimental groups (Group I and II) were anesthestized using a combination of xylazine hydrochlorate (10 mg/kg body weight) (Ketalar, Pfizer İlaçları Limited Şirketi, İstanbul, Turkey) and ketamine hydrochloride (15 mg/kg body weight) (Rompun, Bayer Türk Kimya Sanayi Ltd, Şirketi, İstanbul, Turkey) and were then irradiated under general anesthesia for approximately 30 min. Irradiation was delivered by a ^{60}Co teletherapy unit (Shandong Xinhua SCC-8000S, Shandong Xinhua Medical Instrument Co., Ltd, Shangdong, China) at a dose rate of 0.82 Gy/min. Right legs of rats were irradiated in supine position individually using an anterior 5×5 cm single field with a depth of 0.5 cm with a 2 Gy daily fraction doses for 10 days (total dose = 20 Gy). The fields surrounding the target area were shielded with lead blocks.

After irradiation, the animals were examined daily for disturbances in motor functions. For evaluating motor function, animals were assessed by dragging of extended forelegs or by walking on their forelegs when lifted by the tail.

Electrophysiological measurements were performed in vivo under general anesthesia. The animals were sacrificed by high-dose anesthetization in both groups. The sciatic nerve samples were excised from approximately 1 cm proximal to trifurcation of the sciatic nerve from the right leg. Tissue samples were used for biochemical and histological analyses.

Recordings of Compound motor action potentials (CMAP)

The rats were kept anesthetized and fixed by the frame during the entire procedure for recording of CMAP. CMAP was recorded in control group, Group I and II using standardized nerve conduction study techniques (Aminoff 1998). Data were collected by means of a MP 100 acquisition system (BIOPAC Systems, Inc., Santa Barbara, CA, USA). Bipolar surface electrodes (small bipolar nerve electrodes) (Medelec Ltd, Oxford, UK) were used for stimulation. Surface disc electrodes (Medelec Ltd) were used for recordings from the gastrocnemius muscle. The ground electrode (Medelec Ltd) was placed on thigh on the side of stimulation. The supramaximal stimulus was consisted of single square pulse (intensity 10 V, duration 0.5 ms). In all groups, the point of stimulation was kept constant. Sciatic nerve was stimulated at the level of the sciatic notch. Latency and amplitude of CMAP recordings were measured. Latency is the time in milliseconds from the stimulus artifact to the first negative deflection of CMAP as shown in Figure 1. It is the measure of conduction in the fastest conducting motor nerve fibers. The amplitude of CMAP was measured from the base line to the negative peak (base to peak). The amplitude correlated with the number of nerve fibers. AcqKnowledge analysis software (BIOPAC Systems, Inc., Santa Barbara, CA, USA) was used to measure CMAP latency and amplitude.

Biochemical evaluation

Tissue samples were homogenized (T 25 Ultra-Turrax, IKA Werke GmbH, Staufen, Germany) with 50 mM phosphate buffered salin (PBS) (pH 7,4) (Sigma-Aldrich Chemical Co, St Louis, MO, USA). Then, homogenates were centrifuged (Hettich Mikro 22R, Andreas Hettich GmbH & Co. KG, Tuttlingen, Germany) at 10,000 *g* for 15 min at 4°C. Supernatants were separated and kept at −20°C until enzyme activities and MDA measurements were performed.

Protein in supernatants was determined as described before, using bovine serum albumin as standard (Lowry et al. 1951). Tissue MDA levels, an index of lipid peroxidation, were determined by thiobarbituric acid (TBA) reaction. The

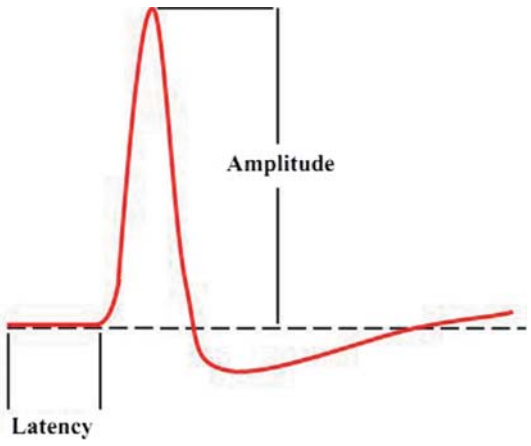

Figure 1. Measurement CMAP amplitude and latency.

Table I. Ultrastructural grading system of myelinated axons.

Grade 0	Normal
Grade 1	Separation in myelin configuration
Grade 2	Interruption in myelin configuration
Grade 3	Honeycomb appearance
Grade 4	Collapsed myelin forming ovoids

color complexes produced by the interaction of TBA (Sigma-Aldrich Chemical Co, MO, USA) with MDA were measured at 532 nm on a spectrophotometer (Varian, Inc., Palo Alto, CA, USA). The colored reaction with 1,1,3,3-tetraethoxy propane (Sigma-Aldrich Chemical Co, MO, USA) was used as the primary standard. MDA levels were determined by a previously defined method of Yagi (1998). MDA levels were expressed as a nanomol per milligram of protein (nmol/mg protein). Tissue CAT activity was measured in supernatants by the method of Aebi (1984). The decomposition of the substrate H_2O_2 was monitored spectrophotometrically at 240 nm. Specific activity was defined as micromole substrate decomposed per minute per milligram of protein (U/mg protein). SOD activity was measured by the inhibition of nitroblue tetrazolium (NBT) (Sigma-Aldrich Chemical Co, MO, USA) reduction due to $O_2^{\cdot -}$ generated by the xanthine/xanthine oxidase system (Sun et al. 1988). One unit of SOD activity was defined as the amount of protein causing 50% inhibition of the NBT reduction rate.

Histological methods

Perfusion fixation was prepared using 4% paraformaldehyde (Merck KGaA, Darmstadt, Germany) and 0.5% gluteraldehyde (Electron Microscopy Sciences, Fort Washington, PA, USA) for electron microscopic examination. Sciatic nerve tissues were cut into small pieces (1 mm^3) and fixed in 2.5% gluteraldehyde (Electron Microscopy Sciences). After fixation, samples were postfixed in osmium tetroxide (Electron Microscopy Sciences), processed routinely for electron microscopy and embedded in resin kit (Electron Microscopy Sciences). Semi-thin sections (1 μm) and ultra-thin sections (70 nm) were cut by a Leica UCT-125 ultramicrotome (Leica Microsystems GmbH, Wien, Austria). Ultrathin sections from selected blocks were mounted on copper grids (Electron Microscopy Sciences), contrasted with uranyl acetate (Electron Microscopy Sciences) and lead citrate (Electron Microscopy Sciences) and were examined with an electron microscope (JEOL-JEM 1011, Jeol Ltd., Tokyo, Japan) and were photographed with a digital camera (Megaview III, Olympus Soft Imaging Solutions GmbH, Münster, Germany) attached to the microscope.

Previously described grading systems were used to evaluate the myelin sheaths (Kaptanoglu et al. 2002) (Table I) and the damaged axons (Erdine et al. 2009) (Table II). Ten samples from each group were analyzed by a quantitative evaluating method. Fifty myelinated axons from each sample and totally 500 myelinated axons from each group were examined ultrastructurally.

Statistical analysis

Distribution of the data has been analyzed with Shapiro-Wilk test. Normally distributed data were analyzed with parametric tests while non-parametric tests were used for the rest. One-way analysis of variance (ANOVA) and Bonferroni post hoc test were used for the comparison of latency and amplitude variables, the mean MDA levels and the mean SOD, CAT activities. Kruskal-Wallis test and Dunn post hoc test were used for the comparison of grading systems of the myelin sheaths and the damaged axons. Differences in histological damage stages were compared with Chi-square test. Values of $p < 0.05$ were considered as statistically significant. Statistical analysis was performed by using SPSS v.11.5 for Windows (SPSS Inc., Chicago IL, USA) and Statistica v.6.1 (StatSoft Inc., Tulsa, OK) statistical packages.

Results

Motor function evaluation

No dragging of extended forelegs or inability to walk was observed in all animals 3 and 6 months after radiation.

Electrophysiology

In Group I and II, the amplitude of CMAP was significantly lower ($p < 0.05$) and the latency was significantly higher ($p < 0.05$) than the control group (Figure 2A and 2B). Amplitude of CMAP in the control group, Group I and Group II was measured as 7.94 ± 1.66 mV, 4.10 ± 0.51 mV and 3.73 ± 1.11 mV, respectively. Latency in the control group, Group I and Group II was measured as 1.58 ± 0.77 ms, 8.96 ± 0.50 ms and 7.37 ± 2.14 ms, respectively. There was no significant differences between Group I and Group II for CMAP amplitude and latency.

MDA level, SOD and CAT activities

Lipid peroxidation and antioxidant statuses of the sciatic nerve after radiotherapy of the irradiated rats were shown in Table III. The MDA levels were increased almost three times, whereas the activities of antioxidizing enzymes SOD and CAT were decreased about two times as a result of radiotherapy

Table II. Scoring of damage to axonal ultrastructure.

Score	Degree of damage	Description of damage
1−	No damage	Mitochondria, microtubules, and microfilaments normal
1+	Low damage	Some vacuole and inclusions, some swelling in the mitochondria; and microtubules and microfilaments normal
2+	Mild damage	Large vacuoles, damaged external membrane and crista, formation of multilaminar structures, and swollen shape of mitochondria; and occasional abnormalities on the microtubules and microfilaments
3+	High damage	The same as in 2+ (mild damage), but in addition large areas of fragmented microtubules and microfilaments, or substantial absence of microtubules

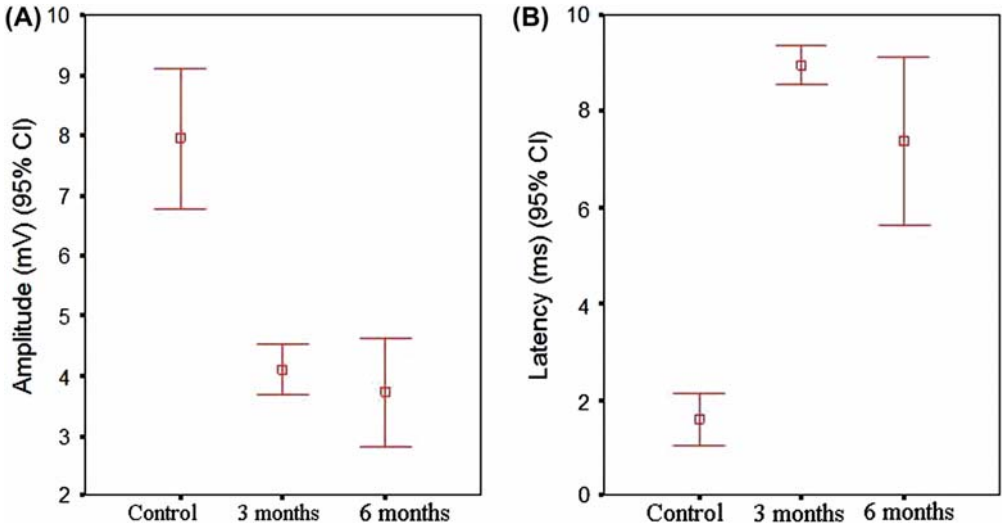

Figure 2. (A) Mean amplitude values of control and experimental groups. CI = confidence interval. Bars represent mean ± standard deviation values. (B) Mean latency control and experimental groups. CI = confidence interval. Bars represent mean ± standard deviation values.

both in Group I and Group II compared with the values in the control group ($p < 0.05$). However, there were no significant changes in these parameters in Group I compared to Group II (MDA levels, activities of enzymes SOD and CAT, $p = 0.09$, $p = 0.11$, $p = 0.06$, respectively).

Electron microscopic evaluation

In the control group, almost all of the myelinated and unmyelinated axons were normal. Myelin sheaths of myelinated nerve fibers had normal structure (Figure 3A). The axoplasm contained well-aligned microtubules and microfilaments with no obvious abnormalities (Figure 3B). The mitochondria were well shaped and its membranes and cristae had normal structure (Figure 3C). Additionally, blood vessels in the endoneurium had also normal appearance (Figure 3D).

In Group I, severe degeneration was observed. Beside the sparse amount of normal myelinated axons, most of the myelinated axons were damaged and degenerated. In slightly damaged fibers; normal appearing axoplasms were surrounded by delaminated and deformated myelin sheaths. In severely damaged or degenerated fibers; myelin sheaths were delaminated and disintegrated (Figure 4A). Disorganization of microfilaments and loss of microtubules were observed in some areas. Mitochondrial swelling and loss of cristae were determined in the axoplasm (Figure 4B and 4C). Additionally, axoplasms were darkened. There were myelin ovoids, vacuoles and centrally oriented organelle accumulations in the axoplasms (Figure 4D). Congestion in blood vessels was also evident in the endoneurium (Figure 4E).

Table III. MDA concentration, CAT and SOD activities in the control and the irradiated groups. Data were represented as mean ± standard deviations.

Variables	Control ($n = 10$)	3 months ($n = 10$)	6 months ($n = 10$)
MDA (nmol/mg protein)	0.5 ± 0.1	1.7 ± 0.9[a]	1.5 ± 0.8[a]
CAT (U/mg protein)	165.6 ± 21.9	89.4 ± 10.5[a]	78.3 ± 9.8[a]
SOD (U/mg protein)	80.5 ± 9.7	40.3 ± 8.5[a]	38.2 ± 7.4[a]

[a]Significantly different from the control at $p < 0.05$.

In Group II, most of the myelinated axons were damaged. Observed damage patterns were myelin sheath delaminations, deformations and interruptions (Figure 5A). Microtubule and microfilament arrays were disrupted, and their intensities were decreased in some areas. Degenerated mitochondria were also observed in axoplasms (Figure 5B and 5C). Some axoplasms were darkened. There were myelin ovoids, vacuoles and centrally oriented organelle accumulations (Figure 5D). Similar to Group I, congestion in blood vessels was observed in the endoneurium (Figure 5E).

Grading of myelin sheaths and damaged axons

Median value of the ultrastructural myelin sheath damage grading was 0 (mean: 0.18) in the control group, 3 (mean: 2.77) in Group I and 3 (mean: 2.62) in Group II. Differences between the control group and Group I, and control group

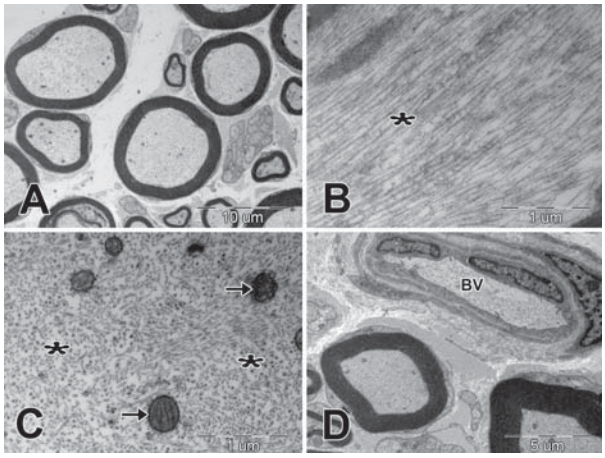

Figure 3. Transmission electron micrographs of the control group. (A) Myelin sheaths and axoplasms of myelinated nerve fibers are ultrastructurally normal (×4,000). (B) Well-aligned microtubules and microfilaments are seen as normal (asterisk). Longitudinal section (×40,000). (C) Mitochondria are normal (arrows), and microtubules and microfilaments are dispersed homogenously (asterisks). Cross section (×40,000). (D) Congestion does not exist in the blood vessel (BV) (×7,500).

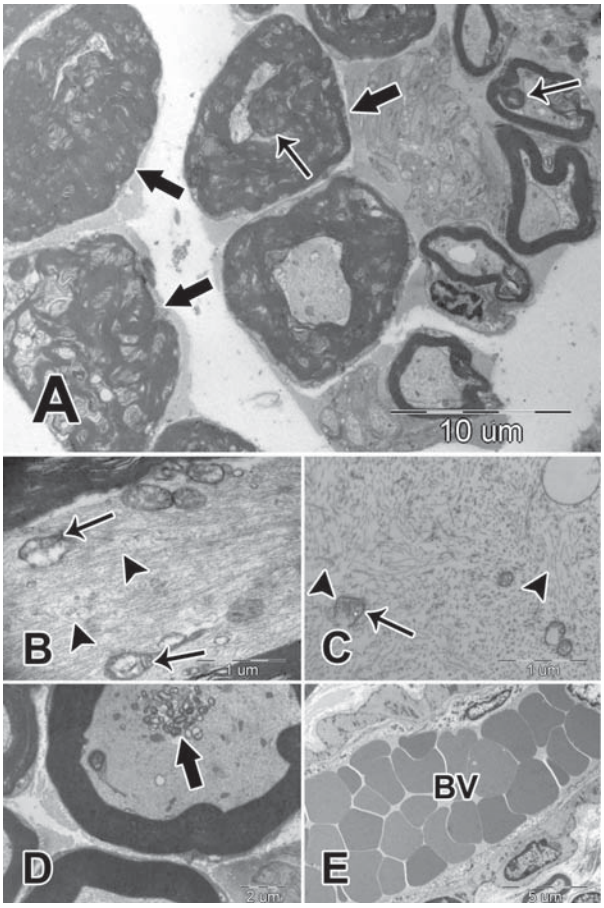

Figure 4. Transmission electron micrographs from Group I. (A) Most of the myelinated axons are shown severely degenerated with myelin sheaths (arrows), myelin ovoids (thin arrows), delamination and deformation in myelin structure (×4,000). (B) Microtubule and microfilament arrays are disorganizated and disrupted (arrowheads). The mitochondria are swollen and damaged (arrows). Longitudinal section (×40,000). (C) Microtubules and microfilaments are dispersed heterogenously. In some areas number of microtubules are decreased (arrowheads). Degenerated mitochondria (arrow). Cross section (×40,000). (D) Vacuolar changes and centrally oriented organelle accumulations (arrow) in a darkened axoplasm (×10,000). (E) Congestion in a blood vessel (BV) (×7,500).

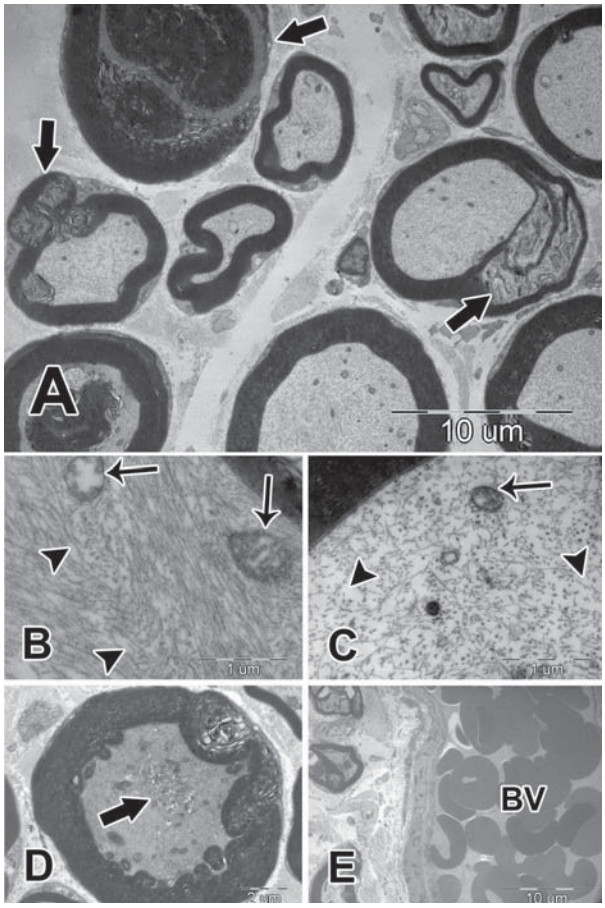

Figure 5. Transmission electron micrographs from Group II. (A) Delamination, deformation and degeneration in myelin sheaths (arrows) (×4,000) (B) Microtubule and microfilament arrays are disrupted (arrowheads). The mitochondria are swollen and deformed, their cristae, inner and outer membranes are deteriorated (arrows). Longitudinal section (×40,000). (C) Microtubules and microfilaments are dispersed heterogenously and devoid of microtubules in some areas (arrowheads). Degenarated mitochondria (arrow). Cross section (×40,000). (D) Axoplasm of the myelinated fiber is darkened and containing myelin ovoids, vacuoles and centrally oriented organelle accumulations (arrow) (×10,000). (E) Congestion in a blood vessel (BV) (×7,500).

and Group II were statistically significant ($p < 0.05$). However, there was no significant difference between group I and group II ($p = 0.06$) (Figure 6A).

Ultrastructural axonal damage score median value was 0 (mean: 0.22) in the control group, 2 (mean: 2.20) in Group I and 2 (mean: 2.12) in Group II. Similar to ultrastructural myelin grading score, there were statistically significant differences ($p < 0.05$) between the control group and Group I, and the control group and Group II, while there was no statistically significant difference between Group I and Group II ($p = 0.12$) (Figure 6B).

Discussion

In the present study, we found that a dose of 20 Gy in 10 fractions radiotherapy induced electrophysiological, biochemical and histological changes in the normal rat sciatic nerve. Changes were observed 3 and 6 months after radiotherapy.

We investigated the effects of fractioned doses of radiation over several days or weeks which is preferred in most clinical situations. We also preferred 20 Gy for simulating the most widely conventional radiation dose. In a clinical study, the neuropathy was observed following the administration of conventional radiotherapy doses. The severity of the neuropathy was found to be related to the size of both the fractions and total dose (Stoll and Andrews 1966, Gillette et al. 1995).

Clinical observations demonstrated that the symptoms of neuropathy may begin 6 months after radiation or may not appear for years; the average interval was calculated as 1–4 years (Stoll and Andrews 1966). De Vrind et al. (1993) reported that high doses of IR (up to 70 Gy) did not lead to functional impairment even after 90 weeks in rats. Lin et al. (2011) stated that motor function tests remained intact in rabbit sciatic nerve recieved 25 Gy single dose by stereotactic radiosurgery (SRS) at 3, 5 and 7 months. Similarly, in the present study, leg weakness was not observed at 3 and 6 months even though there were ultrastructural, electrophysiological and biochemical changes in the sciatic nerve. This parodoxal situation might be due to the crude measures

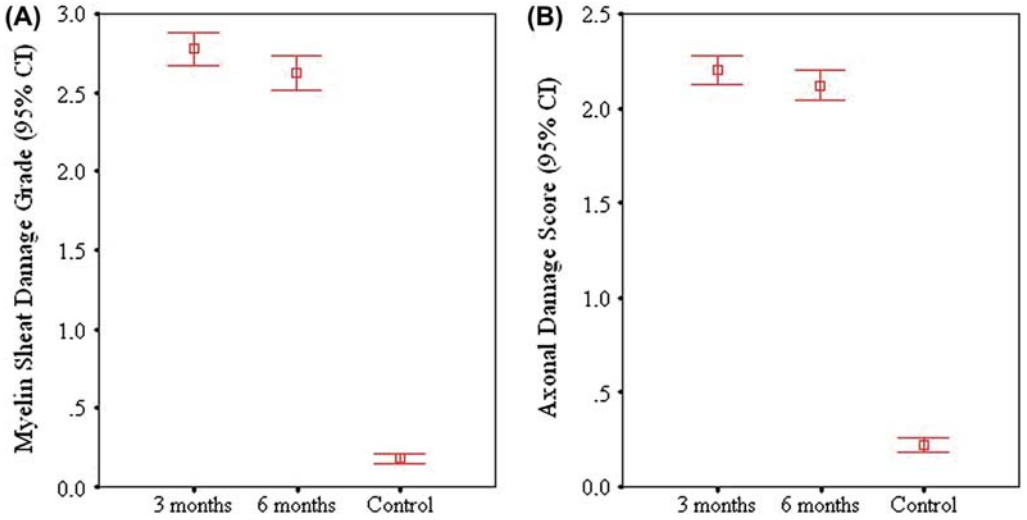

Figure 6. (A) Ultrastructural myelin sheath damage grading of control and experimental groups. CI = confidence interval. Bars represent mean ± standard deviation values. (B) Scoring of damage to axonal ultrastructure in the control and experimental groups. CI = confidence interval. Bars represent mean ± standard deviation values.

used to evaluate motor weakness. This was one of the limitations of the current study.

In our electrophysiological investigation, radiotherapy decreased the CMAP amplitude by 48% and the latency increased 464% 3 months after radiotherapy. Six months after radiotherapy, these values were 53% and 300%, respectively. These electrophysiological findings indicated different patterns of neuropathy, including axonal neuropathy and demiyelinating neuropathy. An axonal neuropathy is characterized by the findings of preserved latency with diminished action potentials. In demyelinating neuropathy, latency is increased while the action potential may be reduced or normal in amplitude (Kimura 2001).

In order to ascertain whether the electrophysiological properties were associated with corresponding alterations in morphological signs of sciatic nerve, ultrastructural examinations were carried out. Ultrastructurally, we observed alterations in the nerve fibers in the 3rd and 6th months. Grading of sciatic nerve damage by transmission electron microscopy supported our ultrastructural histopathological changes. Lin et al. (2011) reported that single fraction radiosurgery (25 Gy) to the rabbit sciatic nerve did not result in histological and ultrastructural changes in the nerve after 3 months. However, mild myelin sheath alterations were observed after 5 months and severe myelin and axonal changes were also observed after 7 months. Inconsistency in the 3rd month between the two studies might be due to receiving the 25 Gy single dose by SRS in the latter study. Due to the isolation from the surrounding tissues, SRS primarily affects the peripheral nerve. While ERBT was used in the present study, it is thought to be effective on both peripheral nerve and surrounding tissues. The IR does not only affect the peripheral nerve, but also causes the release of ROS and inflammatory mediators from the surrounding tissues. Moreover, vascular congestion of endoneureal vessels possibly caused additional harmful effects in the nerve which might be due to secondary production of ROS.

In the present study, we found that the MDA levels in the sciatic nerves of the irradiated groups (Group I and Group II) were significantly higher than those of the control group, which is consistent with the hypothesis that IR generates oxidative stress (Demir et al. 2003, Ustinova and Riabinin 2003). We also found that the SOD and CAT activities in the irradiated groups were lower than those of the control group. Baluchamy et al. (2012) showed that lipid peroxidation was increased and SOD activity was decreased following different doses (0.01, 1 and 2 Gy) of radiation in the mouse nervous system. Guney et al. (2005) reported that MDA levels were increased, while SOD and CAT activities were decreased after 8 and 15 Gy single doses of radiation in guinea pig brains. In another study, it was reported that MDA levels were increased in different tissues of mouse including brain after 4 and 6 Gy single doses of radiation (Manda et al. 2007). Erkal et al. (2006) reported that single dose of 20 Gy radiation increased the levels of MDA and decreased the activities of SOD and CAT enzymes within hours and were leveled out gradually in 48 h in rat brains. In the current study, persistence of high MDA levels and low activity of SOD and CAT enzymes in 3rd and 6th months might be due to the continuing vascular congestion leading ischemic status.

In the present study, congestion was observed in the blood vessels of the endoneurium in the 3rd and 6th months after radiothreapy. The radiation damage to the vascular structures and congestion can cause hypoxia. One of the most significant organelles is the mitochondrium which is affected by hypoxia. Depending on the mechanism of oxidative damage; peroxidation of mitochondrial membrane phospholipids impairs the integrity of external and internal mitochondrial membranes. Loss of cristae and swelling of mitochondria were observed in myelinated axoplasms in the experimental groups. Damage of mitochondria can cause disruption of energy producing processes and blockage of transport of all vesicles along the microtubules (Kaasik et al. 2007). In addition, some of the available experimental data suggest that radiation-induced reorganization and breakdown of different cytoskeletal elements are related to modified calcium homeostasis or altered phosphorylation/dephosphorylation state of proteins in the irradiated cells (Somosy et al. 1995,

Kaptanoglu et al. 2002). As mentioned above, the present ultrastructural axonal and biochemical changes can be related to increased latency and decreased CMAP, respectively. These results indicate that IR can cause oxidative stress increase and anti oxidative capacity decrease.

In conclusion, in the light of our findings, a dose of 20 Gy in 10 fractions radiotherapy causes neuropathic damages in normal sciatic nerve of rats 3 and 6 months after irradiation. Acute, subacute and chronic effects of IR with different doses can be studied for further investigations in the future.

Acknowledgements

The authors are grateful to Vet. Mr Hasan KIRBAS for kindly providing the animals and care for them.

Declaration of interest

The authors report no conflicts of interest. The authors alone are responsible for the content and writing of the paper.

References

Aebi H. 1984. Catalase in vitro. Methods in Enzymology 105:121–126.
Aminoff MJ. 1998. Electromyography in clinical practice. 3rd ed. Edinburgh, UK: Churchill Livingstone.
Baluchamy S, Ravichandran P, Ramesh V, He Z, Zhang Y, Hall JC, Jejelowo O, Gridley DS, Wu H, Ramesh GT. 2012. Reactive oxygen species mediated tissue damage in high energy proton irradiated mouse brain. Molecular and Celluler Biochemistry 360:189–195.
Data K, Sinha S, Chattopadhyay P. 2000. Reactive oxygen species in health and disease. National Medical Journal of India 13:304–310.
de Vrind HH, van Dam WM, Wondergem J, Haveman J. 1993. Latent X-ray damage in the rat sciatic nerve results in delay in functional recovery after a heat treatment. International Journal of Radiation Oncology Biology Physics 63:83–89.
Demir M, Konukoglu D, Kabasakal L, Yelke HK, Ergen K, Ahmed S. 2003. The effects of exposure of 60Co on the oxidant/antioxidant status among radiation victims. Journal of Environmental Radioactivity 64:19–25.
Erdine S, Bilir A, Cosman ER, Cosman ER Jr. 2009. Ultrastructural changes in axons following exposure to pulsed radiofrequency fields. Pain Practise 9:407–417.
Erkal HS, Batcioglu K, Serin M, Uyumlu B, Yücel N. 2006. The evaluation of the oxidant injury as a function of time following brain irradiation in a rat model. Neurochemical Research 31:1271–1277.
Gillette EL, Mahler PA, Powers BE, Gillette SM, Vujaskovic Z. 1995. Late radiation injury to muscle and peripheral nerves. International Journal of Radiation Oncology Biology Physics 31:1309–1318.
Goodhead DT. 1994. Initial events in the cellular effects of ionizing radiations: Clustered damage in DNA. International Journal of Radiation Biology 65:7–17.
Guney Y, Bilgihan A, Hicsonmez A, Dizman A, Ozogul C, Andrieu MN, Kurtman C. 2005. Influence of different doses of irradiation on oxidant and antioxidant systems in the brain of guinea pigs. American Journal of Immunology 1:114–118.
Halliwell B, Gutterage JM. 1990. Role of free radicals and catalytic metal ions in human disease: An overview. Methods in Enzymology 186:1–85.
Iliakis G. 1991. The role of DNA double strand breaks in ionizing radiation-induced killing of eukaryotic cells. BioEssays 13:641–648.
Kaasik A, Safiulina D, Choubey V, Kuum M, Zharkovsky A, Veksler V. 2007. Mitochondrial swelling impairs the transport of organelles in cerebellar granule neurons. Journal of Biological Chemistry 282: 32821–32826.
Kaptanoglu E, Palaoglu S, Surucu HS, Hayran M, Beskonakli E. 2002. Ultrastructural scoring of graded acute spinal cord injury in the rat. Journal of Neurosurgery 97:49–56.
Kimura J. 2001. Electrodiagnosis in disease of nerve and muscle: Principles and practice. 3rd ed. Philadelphia, PA: FA Davis.
Kinsella TJ, Sindelar WF, DeLuca AM, Pezeshkpour G, Smith R, Maher M, Terrill R, Miller R, Mixon A, Harwell JF, Rosenberg SA, Glatstein E. 1985. Tolerance of peripheral nerve to intraoperative radiotherapy (IORT): Clinical and experimental studies. International Journal of Radiation Oncology Biology Physics 11:1579–1585.
Liang BC. 1999. Radiation-associated neurotoxicity. Hospital Physician 35: 54–58.
Lin Z, Wu VWC, Ju W, Yamada Y, Chen L. 2011. Radiation-induced changes in peripheral nerve by stereotactic radiosurgery: A study on the sciatic nerve of rabbit. Journal of Neurooncology 102:179–185.
Lowry OH, Rosenbrough NJ, Farr AL, Randall RJ. 1951. Protein measurement with the folin phenol reagent. Journal of Biological Chemistry 193:265–275.
Manda K, Ueno M, Moritake T, Anzai K. 2007. α-Lipoic acid attenuates X-irradiation-induced oxidative stress in mice. Cell Biology and Toxicology 23:129–137.
Mates JM, Perez-Gomez C, Nunez de Castro I. 1999. Antioxidant enzymes and human diseases. Clinical Biochemistry 32:595–603.
Ruifrok ACC, Kleiboer BJ, van der Kogel AJ. 1992. Fractionation sensitivity of the rat cervical spinal cord during radiation retreatment. Radiotherapy and Oncology 25:295–300.
Ruifrok ACC, Stephens LC, van der Kogel AJ. 1994. Radiation response of the rat cervical spinal cord after irradiation at different ages: Tolerance, latency and pathology. International Journal of Radiation Oncology Biology Physics 29:73–79.
Somosy Z, Sass M, Bognar G, Kovacs J, Köteles GJ. 1995. X-irradiation-induced disorganisation of cytoskeletal filaments and cell contacts in HT29 cells. Scanning Microscopy 9:763–772.
Stoll BA, Andrews JT. 1966. Radiation-induced peripheral neuropathy. British Medical Journal 1:834–837.
Sun C, Redpath JL, Colman M, Stanbridge EJ. 1988. Further studies on the radiation-induced expression of a tumor-specific antigen in human cell hybrids. Radiation Research 114:84–93.
Ustinova AA, Riabinin VE. 2003. Effect of chronic gamma-irradiation on lipid peroxidation in CBA mouse blood serum. Radiation Biology Radioecology 43:459–463.
van der Kogel AJ. 1977. Radiation-induced nerve root degeneration and hypertrophic neuropathy in the lumbosacral spinal cord of rats: The relation with changes in aging rats. Acta Neuropathologica 39:139–145.
Yagi K. 1998. Simple procedure for specific enzyme of lipid hydroperoxides in serum or plasma. Methods in Molecular Biology 108:107–110.